UCRL-JC-121197
PREPRINT
CONF-9505264--12

Efficient Broadband Third Harmonic Frequency Conversion Via Angular Dispersion

D. M. Pennington, M. A. Henesian,
D. Milam, and D. Eimerl

This paper was prepared for submittal to the
1st Annual International Conference on Solid-State Lasers for
Application to Inertial Confinement Fusion
Monterey, CA
May 30 - June 2, 1995

July 18, 1995

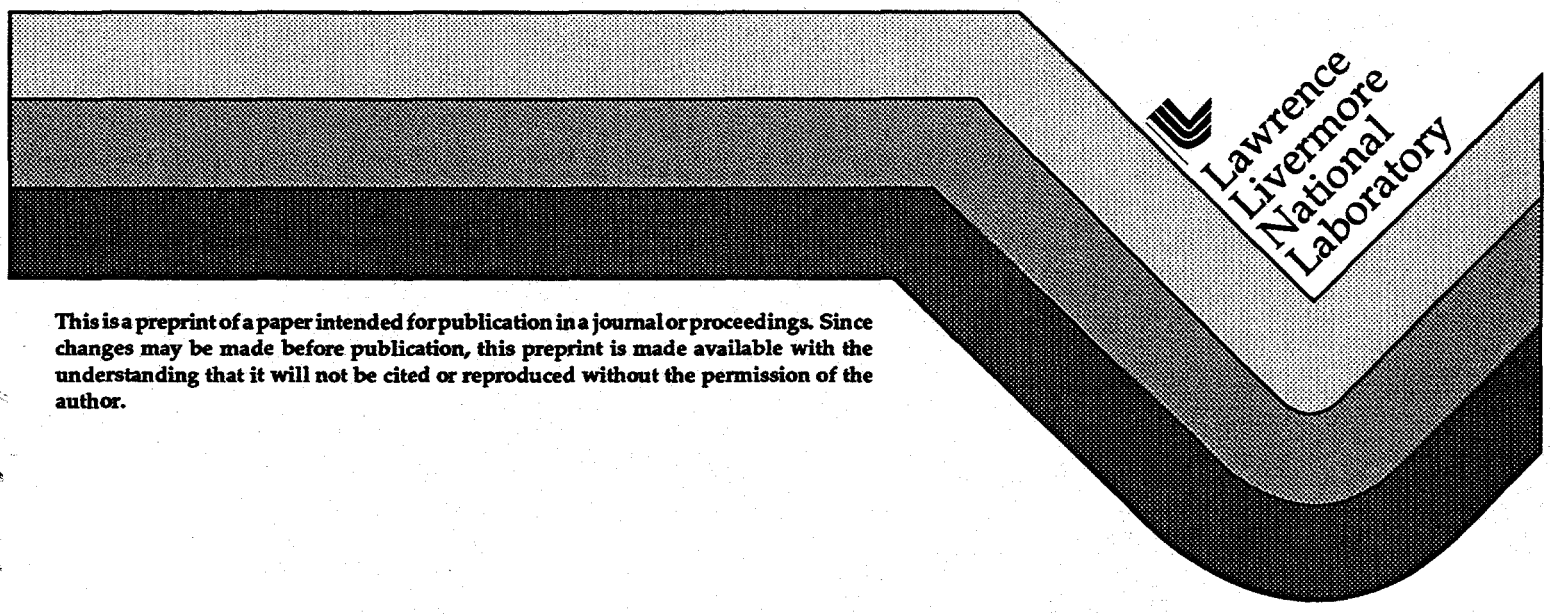

DISCLAIMER

EFFICIENT BROADBAND THIRD HARMONIC FREQUENCY CONVERSION VIA ANGULAR DISPERSION

D. M. Pennington, M. A. Henesian, D. Milam, D. Eimerl
Lawrence Livermore National Laboratory
Laser Program
P.O. Box 5508, L-493
Livermore, CA 94551-9900

ABSTRACT

In this paper we present experimental measurements and theoretical modeling of third harmonic (3ω) conversion efficiency with optical bandwidth. Third harmonic conversion efficiency drops precipitously as the input bandwidth significantly exceeds the phase matching limitations of the conversion crystals. For Type I/Type II frequency tripling, conversion efficiency begins to decrease for bandwidths greater than ~ 60 GHz. However, conversion efficiency corresponding to monochromatic phase-matched beams can be recovered provided that the instantaneous propagation vectors are phase matched at all times. This is achieved by imposing angular spectral dispersion (ASD) on the input beam via a diffraction grating, with a dispersion such that the phase mismatch for each frequency is zero. Experiments were performed on the Optical Sciences Laser (OSL), a 1-100 J class laser at LLNL. These experiments used a 200 GHz bandwidth source produced by a multipassed electro-optic phase modulator. The spectrum produced was composed of discrete frequency components spaced at 3 GHz intervals. Angular dispersion was incorporated by the addition of a 1200 gr/mm diffraction grating oriented at the Littrow angle, and capable of rotation about the beam direction. Experiments were performed with a pulse length of 1-ns and a 1ω input intensity of ~ 4 GW/cm^2 for near optimal dispersion for phase matching, 5.2 μrad/GHz, with 0.1, 60, and 155 GHz bandwidth, as well as for partial dispersion compensation, 1.66 μrad/GHz, with 155 GHz and 0.1 GHz bandwidth. The direction of dispersion was varied incrementally 360° about the beam diameter. The addition of the grating to the beamline reduced the narrowband conversion efficiency by approximately 10%. Sufficient dispersion to allow nearly full phase-matching of all frequency components along the sensitive axis of the tripler allowed recovery of the narrow band conversion efficiency with bandwidth. However, even partial dispersion compensation was shown to significantly increase broadband 3ω conversion efficiency.

Keywords: broadband frequency conversion, third harmonic generation, angular spectral dispersion

1. INTRODUCTION

For the past few years optical smoothing of the laser irradiance on targets for inertial confinement fusion (ICF) has been given increasing attention.[1-5] Wavefront aberrations in high power laser systems for ICF produce nonuniformities in the energy distribution of the focal spot that can significantly degrade the coupling of energy into a fusion target, driving various plasma instabilities.[6-8] The introduction of temporal and spatial incoherence over the face of the beam, using techniques such as induced spatial incoherence (ISI)[1] or smoothing by spectral dispersion (SSD)[2], reduces variations in the focal irradiance when averaged over a finite time interval. The rate and level of smoothing obtained by use of the SSD technique are strongly dependent on the amount of dispersion and spectral bandwidth a high power laser chain can support. The larger the bandwidth (i.e., the shorter the coherence time), the more rapidly the structure will change, and the more rapidly the time-averaged intensity will smooth. However, high efficiency tripling can be achieved only over a narrow spread in wavelength for a given crystal phase matching condition, thus in order to remain within 10% of the maximum conversion efficiency the input bandwidth is effectively limited to < 60 GHz. Figure 1 demonstrates that the normalized 3ω conversion efficiency drops significantly as the input bandwidth exceeds the phase-matching limitations of the KDP crystals.[5] The data was taken both on Nova and in the OSL using a Type I/Type II conversion scheme, which was chosen because of its increased performance and adaptability to angle tuning[5,9].

In this paper, we will discuss experiments demonstrating that full narrowband conversion efficiency can be recovered with bandwidth by implementing angular spectral dispersion (ASD) along the sensitive axis of the tripler. Use of angular spectral dispersion to improve phase matching of broadband light in the frequency conversion process was first investigated by Volosov, et al.[10-12], for the case of second harmonic generation, and more recently for third harmonic

generation[13,14]. In the case of the latter experiments by Skeldon, et al., insufficient dispersion was used to compensate for phase-matching of the full bandwidth, thus only a partial improvement in 3ω conversion efficiency was observed.[14] We have extended this work to demonstrate full recovery of 3ω conversion efficiency when full dispersion compensation is used. We have also developed a computational approach, that appears to be more general than previous approaches[13,14], which has been used to model the statistical bandwidth (XPM) cases shown in Fig. 1.[5]

The technique of angular spectral dispersion is based on the idea that conversion efficiency corresponding to monochromatic phase-matched beams can be recovered in many circumstances, provided that the instantaneous propagation vectors are phase-matched at all times. This can be achieved by propagating the beam through a dispersive medium, such as a prism or diffraction grating, which causes each frequency to have a different propagation direction. By choosing the grating dispersion to match the crystal material dispersion in the phase matching direction, each frequency can be deflected to phase-match in the crystal, allowing efficient frequency tripling. Full dispersion compensation can provide full recovery of the narrowband conversion efficiency, however, even partial dispersion compensation, can significantly improve broadband conversion efficiency. Full recovery of conversion efficiency using the ASD technique is limited primarily by the divergence that can be tolerated in the laser amplifier chain.

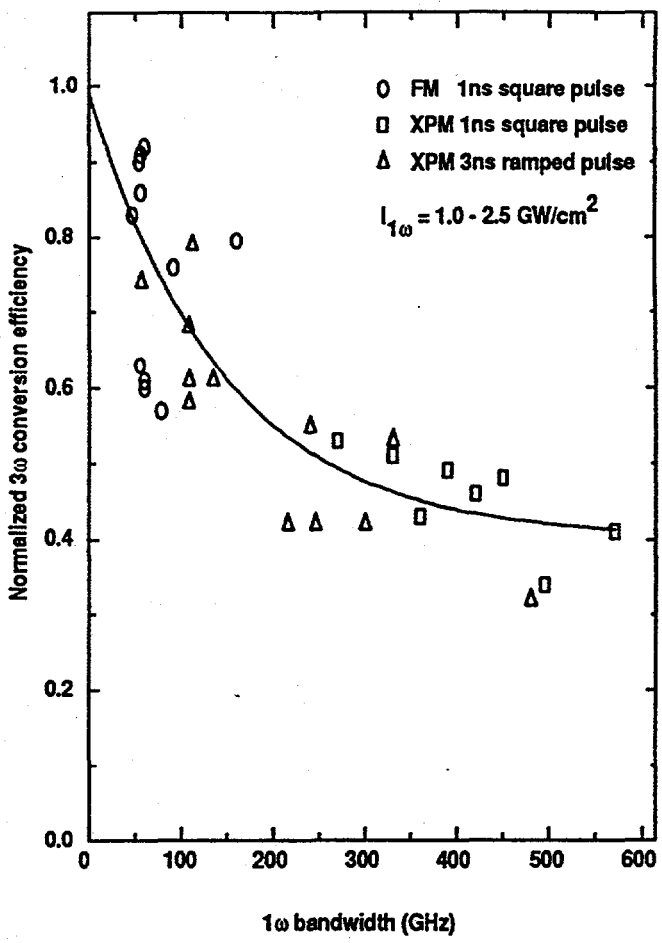

Fig. 1: Data taken in the OSL and on Nova demonstrates that 3ω conversion efficiency drops significantly when the bandwidth exceeds the phase-matching limitations of the crystal.

2. THEORY

High-efficiency harmonic generation in crystals is possible when the three electric field vectors simultaneously satisfy the conditions for conservation of frequency and momentum

$$\omega_1 + \omega_2 = \omega_3 \tag{1}$$

$$\vec{k}_1 + \vec{k}_2 = \vec{k}_3. \tag{2}$$

For broadband lasers, frequency conversion is a large number of simultaneous three-wave interactions. Here the conservation conditions become

$$(\omega_1 + \delta\omega_1) + (\omega_2 + \delta\omega_2) = (\omega_3 + \delta\omega_3) \tag{3}$$

$$(\vec{k}_1 + \delta\vec{k}_1) + (\vec{k}_2 + \delta\vec{k}_2) = (\vec{k}_3 + \delta\vec{k}_3). \tag{4}$$

Frequency must be conserved, therefore $\delta\omega_1 + \delta\omega_2 = \delta\omega_3$. However, some momentum mismatch is tolerable, as long as $\Delta k << \pi/l_c$, where l_c is the crystal length. Therefore, for nominally collinear beams, the momentum mismatch is

$$\Delta k = \delta k_3 - \delta k_2 - \delta k_1 = \left[\frac{\partial k_3}{\partial \omega_3}\delta\omega_3 - \frac{\partial k_2}{\partial \omega_2}\delta\omega_2 - \frac{\partial k_1}{\partial \omega_1}\delta\omega_1\right] = \left[\frac{\delta\omega_3}{v_{g3}} - \frac{\delta\omega_2}{v_{g2}} - \frac{\delta\omega_1}{v_{g1}}\right], \quad (5)$$

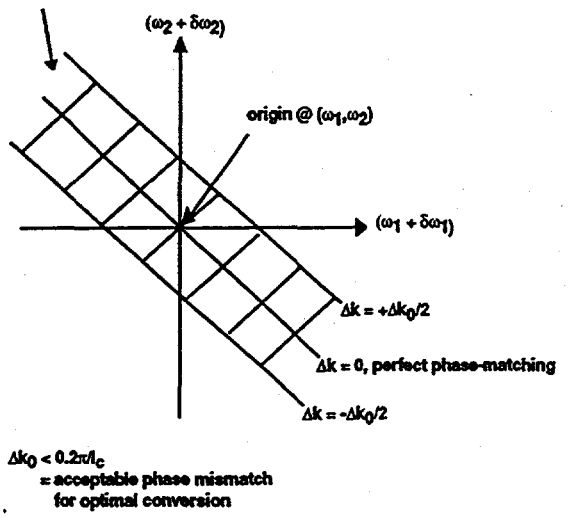

Fig. 2: For broad bandwidth there is a region over which adequate phase-matching can be achieved to allow efficient 3ω frequency conversion.

where v_{g_i} are the group velocities for each wave vector. This provides a region in $(\delta\omega_1,\delta\omega_2)$ space of adequate phase matching for frequency conversion, as shown in Fig. 2. The limited region of the Δk-pass band can be increased by the implementation of angular spectral dispersion. Use of a grating, or other dispersive element applies a compensating phase mismatch to each field, allowing efficient frequency conversion for each frequency.

For a dispersed phase-matched beam with frequency ω_o, propagating along the z-axis as shown in Fig. 3, the wave vector is given by

$$\vec{k} = \frac{\omega_o n(\omega_o,\theta)}{c}\hat{z}, \quad (6)$$

where θ is the angle of propagation relative to the crystal c-axis (not shown). For a frequency $\omega_o + \delta\omega$, the angularly dispersed beam propagates at an angle $\delta\theta$ to the z-axis with wave vector

$$\vec{k}' = \frac{(\omega_o + \delta\omega)n(\omega_o + \delta\omega, \theta + \delta\theta)}{c}\hat{z}'. \quad (7)$$

Thus the longitudinal phase-mismatch along the integration direction through the crystal is

$$\Delta k = (\vec{k}' - \vec{k})\cdot\hat{z}. \quad (8)$$

A power series expansion of Eq. 7 for each field gives

$$\Delta k_1 \cdot \hat{z} = \frac{1}{v_g'}\cdot\delta\omega_1 + \frac{1}{2}k_2'\cdot\delta\omega_1^2, \quad (9)$$

where the reciprocal group velocity is

$$\frac{1}{v_g'} = \left(\frac{1}{v_g}\right)_{material} + \left(\frac{\omega_o}{n_o c}\left(\frac{\partial n}{\partial\theta}\right)_{\theta_o}\cdot\left(\frac{\partial\theta}{\partial\omega}\right)\cdot\sin\psi\right)_{grating} \quad (10)$$

and the group velocity dispersion is

$$k_2' = (k_2)_{material} + \left(\frac{2}{n_o c}\left(\frac{\partial n}{\partial\theta}\right)_{\theta_o}\cdot\left(\frac{\partial\theta}{\partial\omega}\right)\cdot\sin\psi - \frac{\omega_o}{n_o c}\left(\frac{\partial\theta}{\partial\omega}\right)^2\sin^2\psi\right)_{grating}. \quad (11)$$

Here, ψ is the angle of dispersion relative to the ordinary axis of the crystal, as shown in Fig. 3, the spectral dispersion at the crystal is $\left(\frac{\partial\theta}{\partial\omega}\right)$ in units of rad/(2πHz), and $\left(\frac{\partial n}{\partial\theta}\right)_{\theta_o}$ is the crystal angular dispersion, i.e., the change in index with propagation direction relative to the c-axis of the crystal. Therefore, the overall mismatch is:

$$\Delta k = \Delta\vec{k}\cdot\hat{z} = \left(\vec{k}_3 - \left(\vec{k}_1 + \vec{k}_2\right)\right)\cdot\hat{z} + \left(\Delta\vec{k}_3 - \left(\Delta\vec{k}_1 + \Delta\vec{k}_2\right)\right)\cdot\hat{z}. \quad (12)$$

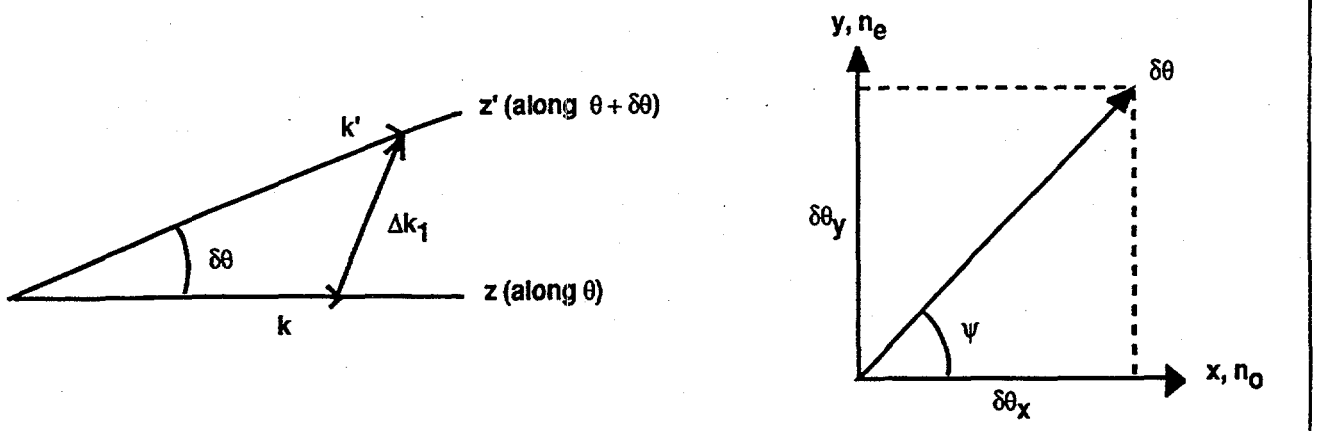

Fig. 3: For a dispersed phase-matched beam with frequency ω_o, propagating along the z-axis the wave vector is given by $\vec{k}$. For a frequency $\omega_o + \delta\omega$, the angularly dispersed beam propagates at an angle $\delta\theta$ to the z-axis with wave vector $\vec{k}'$, as shown on the left. The longitudinal phase-mismatch along the integration direction through the crystal is $\Delta k = (\vec{k}' - \vec{k}) \cdot \hat{z}$. The angle of dispersion, ψ, relative to the ordinary crystal axis (x,n_o) is shown in the plane transverse to the z-axis, as shown on the right.

Phase matching occurs when the grating dispersion is chose such that it compensates for the material dispersion, i.e., when $\Delta k = (\Delta k)_{material} + (\Delta k)_{grating} < \Delta k_o / 2$. The grating modifies the phase of the electric field such that

$$\phi = (kz - \omega t) \rightarrow (kz - \omega t) + k(\frac{\partial \theta}{\partial \omega}\delta\omega)x \ , \tag{13}$$

thus along the z-direction

$$dk_1 \rightarrow \frac{\partial k_1}{\partial \omega_1}\delta\omega_1 + \left(\frac{\partial k_1}{\partial \theta}\frac{\partial \theta}{\partial \omega_1}\right)\delta\omega_1 + O\left(\delta\omega_1^2\right) + \ldots \ . \tag{14}$$

Assuming $\omega_1 = \omega_2 / 2 = \omega_3 / 3$, phase matching of all frequencies in Eq. 12 occurs when

$$\left(\frac{d\theta}{d\omega}\right) = -\left(\frac{d\Delta k}{d\omega} \Big/ \frac{d\Delta k}{d\theta}\right). \tag{15}$$

Using the values for $\frac{d\Delta k}{d\omega}$ and $\frac{d\Delta k}{d\theta}$ for 3ω generation in Type II KDP at λ_o = 1053 nm,[14] the optimal dispersion for phase matching is 6.1 μrad/GHz. The dispersion required to phase match all frequencies in a Type I doubler is neglected since ($d\theta/d\omega$) is 31 times smaller than for a Type II tripler. We developed a broadband frequency conversion code to model our experiments.[5] Broadband frequency conversion is treated as three-wave mixing in a dispersive birefringent nonlinear medium. The coupled nonlinear Schrodinger equations are solved for each of the three fields in each conversion step using a split-operator approach.[16] The z-integration is performed using Runge-Kutta, while the time-integration is performed using a spectral decomposition method. Several third order nonlinear refractive effects, such as self-phase modulation, cross-phase modulation, and two-photon absorption, were included. Spectral dispersion (ASD) effects are included as additional terms to order $O(\delta\omega^2)$ in the group velocity walk-off and dispersion applied to each field, as shown by Eqs. 10 and 11, as well as overall angle and central frequency tuning. The effect of the incident pulse shape on conversion efficiency was included. This model was used to predict the effect of varying dispersion on 3ω conversion efficiency with FM bandwidth pulses, as shown in Fig 4. The calculations were performed for input bandwidths of 160 and 320 GHz, assuming an input intensity of 4 GW/cm^2, a 1 ns pulse length, doubler detuning of 245 μrad, a tripler detuning of 15 μrad, 1% loss/surface, a 10.5 mm thick Type I doubler, and an 8.1 mm Type II tripler. The

results verify that 6.1 μrad/GHz is the optimal dispersion for efficient broadband frequency conversion under these conditions. Additional simulations were performed using the same input parameters to determine if less than optimal dispersion would still provide an increase in broadband conversion efficiency. The simulation results shown in Fig. 5 indicate that for 320 GHz of input bandwidth, even a fraction of the optimal dispersion should significantly improve the 3ω conversion efficiency.

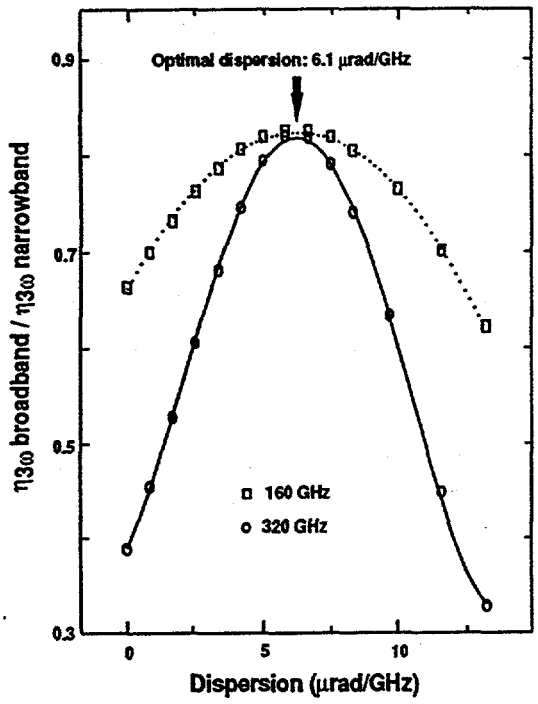

Fig. 4: A broadband frequency conversion code was developed to predict the effect of varying dispersion on broadband 3ω conversion efficiency. The optimal dispersion for efficient broadband conversion at 1053 nm in Type II KDP tripler is 6.1 μrad/GHz.

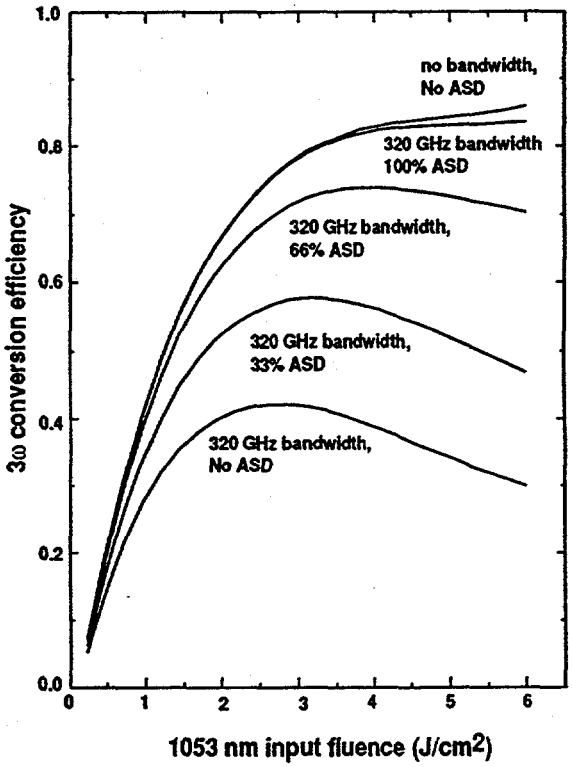

Fig. 5: Simulations indicate that for 320 GHz of input bandwidth, even a fraction of the optimal dispersion should significantly improve the 3ω conversion efficiency

3. EXPERIMENT

The experimental set-up used to test the effect of ASD on frequency tripling with bandwidth in the OSL is shown in Fig. 6. The bandwidth for testing the recovery of conversion efficiency with bandwidth, was produced by a multipassed[16] 3 GHz lithium niobate electro-optic phase modulator. The bandwidth increase per pass, 50 GHz, was approximately equal to the bandwidth obtained from single pass usage. The modulator was positioned in a linear cavity at the output of the pulse shaping system. The pulse transmitted by the pulse shaper passed through a horizontally oriented polarizer, a 45° rotator, a passive Faraday rotator that returns the polarization to horizontal, a second polarizer, a 1-cm Nd:glass amplifier, and a second quarter-wave plate. Upon reflection, the beam polarization was switched to vertical by a second pass through the quarter-wave plate, and was reflected into the multipass cavity by two polarizers. The principle elements in the modulator cavity are the modulator, a quarter-wave plate, and a Pockels cell. Two-pass operation was allowed when the Pockels cell was not fired. The quarter-wave plate first rotates the polarization of the injected pulse to horizontal, keeping the pulse within the cavity, then rotates the polarization to vertical on the second pass to allow reflection of the pulse out of the cavity. This configuration was used during alignment operations to allow circulation of the laser beam through the cavity. Multiple passes were possible when a quarter-wave voltage was applied to the Pockels cell after the first pass of the pulse through the quarter-wave plate. Alignment of the polarization with the

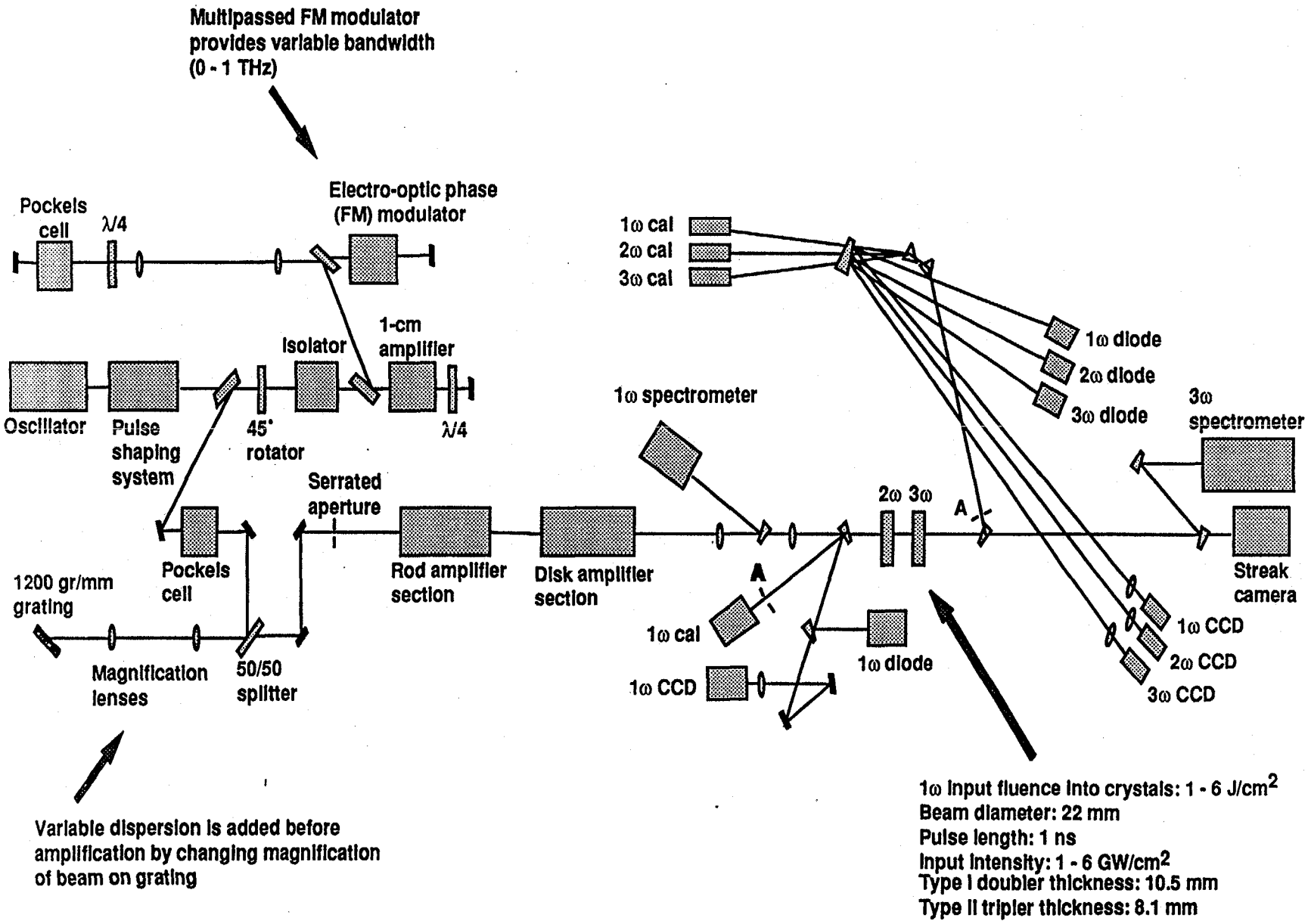

Fig. 6: The experimental set-up used to test the effect of ASD on frequency tripling in the OSL

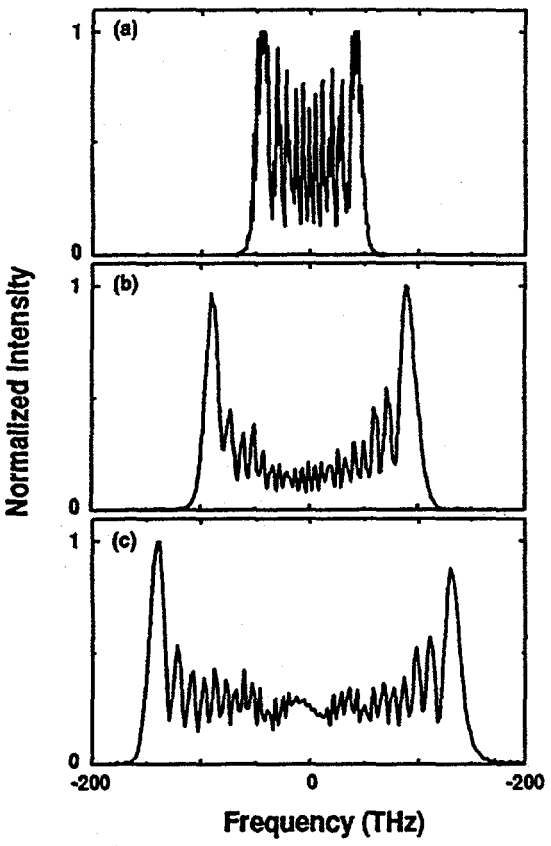

Fig. 7: (a) An example of the 160 GHz spectral envelope produced by the multipassed modulator. (b) Bandwidth doubles upon conversion to the second harmonic, as theoretically expected. (c) The bandwidth approximately triples upon conversion to the third harmonic; however, for the 160 GHz input spectrum, shown in (a), the 3ω bandwidth is beginning to show some narrowing due to phase-mismatch in the tripler.

c-axis of the modulator crystal was maintained because the pulse passed through a polarizer immediately prior to entry into the modulator. Beam size was maintained during multiple passes by two 50 cm lenses that imaged one cavity mirror onto the other.

Progressive accumulation of bandwidth occurs during multiple passes if the phase of the rf field is the same each time the laser pulse arrives at the modulator. Since the laser pulse propagates 10 cm during one rf cycle, the round trip distance between the modulator and the either cavity mirror must be a multiple of this distance. The main limit on the number of passes that can be obtained is passive loss in the cavity. Approximately 40% transmission was obtained for 14 passes. This loss was compensated for by two additional passes through the 1-cm rod amplifier, as shown in Fig. 6. Four passes were used to provide the 155 GHz spectrum used in these experiments. An example of the spectral envelope produced by the modulator is shown in Fig. 7(a). The spectrum is actually composed of discrete frequency components spaced at 3 GHz intervals, though limited instrument resolution precludes observation of the individual components. The experimental spectrum shown in Fig. 7(b) confirms that a 160 GHz input bandwidth doubles upon conversion to the second harmonic, as theoretically expected. Upon conversion to the third harmonic, the bandwidth triples for bandwidths up to 150 GHz and fluences to 6 J/cm^2. For the 160 GHz input spectrum shown in Fig. 7(c), the 3ω bandwidth shows some narrowing due to phase-mismatch in the tripler.

Angular spectral dispersion was added to the beam following the addition of bandwidth. Angular dispersion was incorporated by the addition of a 1200 gr/mm diffraction grating oriented at the Littrow angle to avoid loss and beam distortion. The grating was mounted such that it was capable of rotation about the beam direction. Thus direction of dispersion could varied incrementally 360° about the beam diameter. The degree of ASD was varied by changing the magnification of the beam on the grating. Amplitude modulations were minimized by placing the grating in an image plane, and beam relaying was maintained by the two lenses used for magnification. Experiments were performed for reduced dispersion, 1.66 μrad/GHz, with 155 GHz and 0.1 GHz bandwidth, and for close to optimal dispersion for phase matching, 5.2 μrad/GHz, with 0.1, 60, and 155 GHz bandwidth. Following the addition of dispersion, the beam was amplified in a series of amplifiers to obtain an effective gain of 10^7-10^8. The resulting beam was 22-mm in diameter with a 1-ns pulse length and a 1ω input intensity of ~ 4 GW/cm^2. The beam was frequency converted using a 10.5 mm thick KDP doubler and an 8.1 mm thick KDP tripler. Crystal surfaces were polished following diamond turning to reduce amplitude modulation on the 3ω beam. A 1ω/2ω-compromise coating of sol-gel silica with a silicone undercoat applied to both surfaces of the doubler and to the input surface of the tripler and a 3ω optimized sol-gel coating applied to the output face of the tripler produced a combined transmission at all three harmonics of 85-90%. The crystals were angularly aligned by rocking experiments at high power, 4-5 GW/cm^2 for the doubler, and 1.8 GW/cm^2 for the tripler. The doubler was detuned by 245 – 15 μrad from the optimal 2ω phase-matching angle.

Calorimetry was performed on the 1ω and 3ω beams over the central 13 mm of the beam to eliminate regions of varying intensity in the skirt of the beam. This was accomplished by independently aperturing each beam before the Scientec 38-0111 calorimeters, being careful to sample the same region of the beam in both cases. The calorimeters were fed by paths that contained only bare fused silica wedges, and all beams had either horizontal or vertical polarization so the percent of each pulse that arrived at each calorimeter could be accurately calculated from measurements of the incident angles. The pulse shape was recorded before and after frequency conversion via fast photodiodes and SDC5000 oscilloscopes with a resolution of approximately 3 GHz. bandwidth. Beam profiles were recorded for each wavelength before and after conversion by Cohu 4800 CCD cameras. The spatial quality of the beam was not observed to vary with bandwidth. The bandwidth was measured following amplifications by a 1-m spectrometer with a 1200 gr/mm grating. The output was magnified by a factor of 6 and recorded on a CCD camera.

4. RESULTS AND DISCUSSION

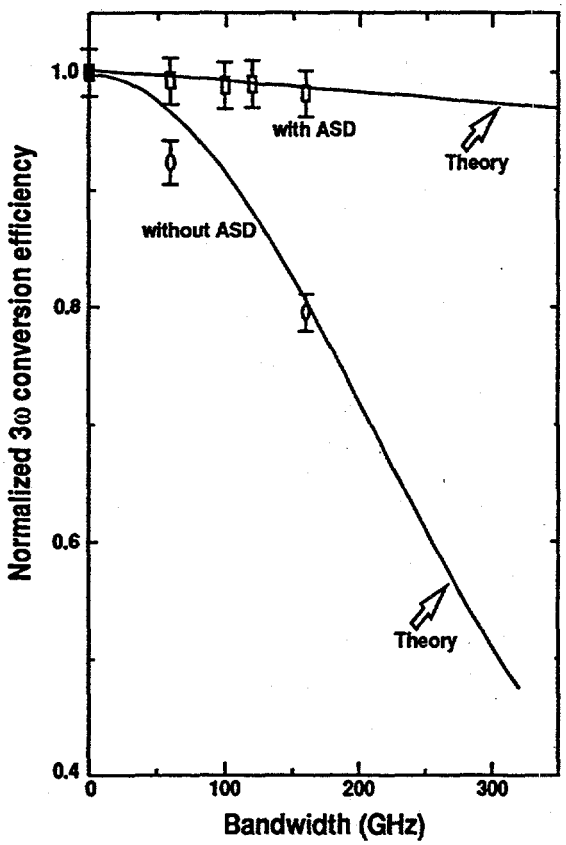

Fig. 8: 3ω conversion efficiency is plotted for varying bandwidth up to 155 GHz for an undispersed beam, and for a beam with nearly full dispersion compensation, i.e., 5.2 μrad/GHz, or 84% compensation. Experimental data is indicated by symbols, while the curves are the result of theoretical calculations.

Three experiments were performed to investigate the effect of ASD on broadband 3ω conversion efficiency. In the first experiment, the 3ω conversion efficiency was measured for varying bandwidth up to 155 GHz for an undispersed beam, and for a beam with nearly full dispersion compensation, i.e., 5.2 μrad/GHz, or 84% compensation. Experiments were performed using a 1-ns nominally square pulse and a 1ω input intensity of 4 GW/cm^2. The results of this experiment, shown in Fig. 8, demonstrate that narrowband conversion efficiency can be recovered with nearly full ASD compensation. Experimental data is indicated by symbols, while the curves are the result of theoretical calculations. Without ASD the conversion efficiency drops by ~20% with the addition of 155 GHz of bandwidth. Implementation of ASD brings the 3ω efficiency back to the narrowband levels to within the experimental error bars. The maximum bandwidth used for these experiments was limited to 155 GHz due to the angular acceptance of the laser chain. It should be noted that upon adding a grating to the narrowband beam, the narrowband conversion efficiency dropped by 10% to 72%. This is most likely caused by amplitude modulation imposed on the beam by the surface quality of the dispersion grating. The experimental data was modeled using the broadband frequency conversion code discussed above. The input parameters assumed in the code were, a doubler detuning of 245 ± 15 μrad, a tripler detuning of ± 15 μrad, 2% loss per surface, a double thickness of 10.5 mm and a tripler thickness of 8.1mm. A ramped 1-ns pulse shape was simulated to match the experimentally measured pulse shape. Theoretical calculations are in good agreement with the data, corroborating the expected recovery of narrowband efficiency with the optimal level of ASD.

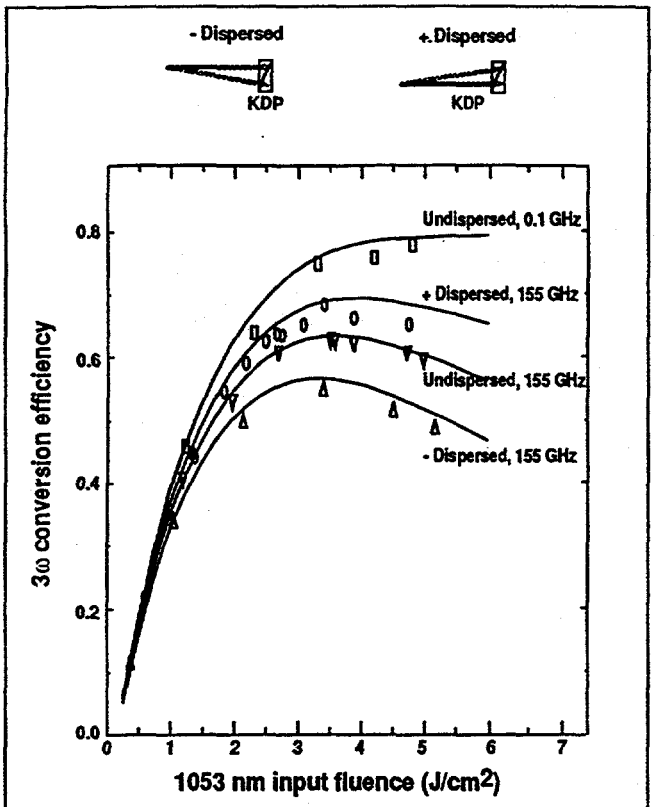

Fig. 9: 3ω conversion efficiency is plotted as a function of input fluence for an undispersed narrowband beam, an undispersed beam with 155 GHz of FM bandwidth, and for 155 GHz bandwidth with the direction of the dispersion oriented such that it improved phase-matching (+ dispersion) and for dispersion rotated 180° out of phase matching (- dispersion). The curves through the data were generated using the broadband frequency conversion code.

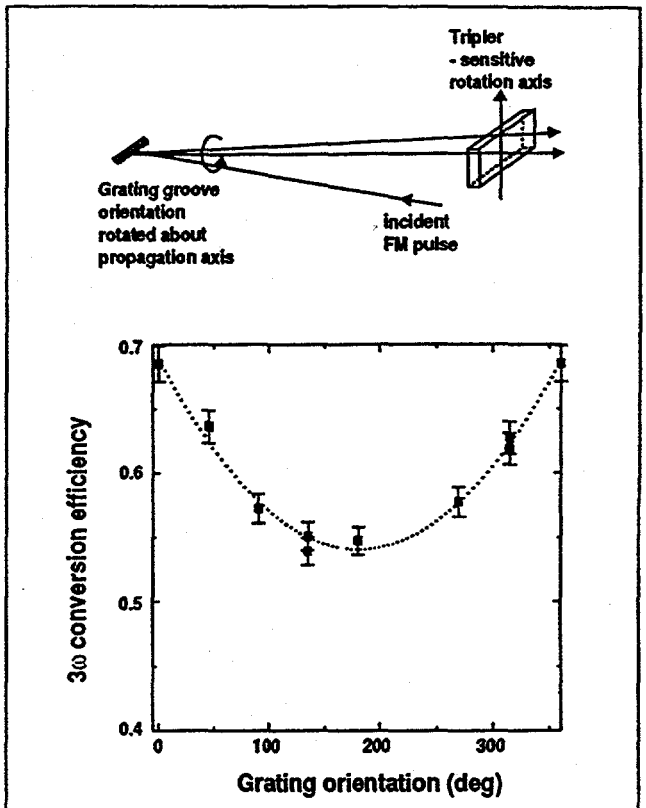

Fig. 10: 3ω conversion efficiency is plotted as a function of dispersion orientation for input intensities between 2.7 and 3.8 GW/cm^2, 160 GHz bandwidth, and 1.66 μrad/GHz dispersion. The dotted curve is a guide to the eye.

The results of the second experiment using a partial dispersion value of 1.66 μrad/GHz are shown in Fig 9. This corresponds to 27% of the optimal dispersion required for phase-matching. The 3ω conversion efficiency (3ω energy out/1ω energy in) is plotted as a function of input fluence for an undispersed narrowband beam, an undispersed beam with 155 GHz of FM bandwidth, and for 155 GHz bandwidth with the direction of the dispersion oriented such that it improved phase-matching (+ dispersion) and for dispersion rotated 180° out of phase matching (- dispersion). All experiments were performed with 1 ns square input pulses. The curves through the data were generated using the broadband frequency conversion code. The input parameters assumed in the code were, a doubler detuning of 245 ± 15 μrad, a tripler detuning of ± 15 μrad, 2% loss per surface, a double thickness of 10.5 mm and a tripler thickness of 8.1 mm. A ramped 1-ns pulse shape was simulated to match the experimentally measured pulse shape. A 3ω conversion efficiency of 76-78% was measured for the undispersed narrowband experiments, in good agreement with the theoretical predictions. When 155 GHz of bandwidth was added, the conversion efficiency was reduced to 60-62%. This drop was partially recovered by the implementation of partial dispersion compensation, resulting in 65-66% conversion efficiency. Experiments performed with the bandwidth negatively dispersed exacerbated the phase-mismatch, reducing the frequency conversion to 52-54%. All four data sets are in good agreement with theoretical prediction.

The third set of experiments was designed to characterize the effect of dispersion direction relative to the sensitive axis of the tripler. The grating was mounted in such a way to allow rotation of the dispersion about the propagation axis as shown in Fig 10. The 3ω conversion efficiency was measured as a function of dispersion orientation for input intensities

between 2.7 and 3.8 GW/cm^2, 160 GHz bandwidth, and a dispersion of 1.66 μrad/GHz. The data shows that to maximize the dispersion compensation, the grating dispersion must be oriented to within ~ 10° of the position for optimal phase matching. The dotted curve shown on the plot is a guide to the eye. The data is in good agreement with the theoretical predictions shown in Fig. 4, and further modeling is in process.

5. SUMMARY

We have demonstrated that efficient third harmonic frequency conversion can be achieved with bandwidth using angular spectral dispersion. The maximum bandwidth and ASD that can be used is determined by the angular acceptance of a given laser chain. Experiments with 155 GHz of bandwidth and sufficient dispersion to allow nearly full phase-matching of all frequency components along the sensitive axis of the tripler allowed recovery of the narrow band conversion efficiency with bandwidth. Also, the implementation of partial ASD compensation can improve broadband 3ω conversion efficiency significantly. Experimental results are in good agreement with theoretical modeling. While our experiments went only to a maximum bandwidth of 160 GHz, theoretical simulations indicate that ASD should be effective for bandwidths greater than at least 320 GHz at 1ω.

6. REFERENCES AND NOTES

This work was performed under the auspices of the U. S. Department of Energy by the Lawrence Livermore National Laboratory under contract number W-7405-ENG-48.

1. S. P. Obenschain, *et al.*, Phys. Rev. Lett., vol. 56, 1986, pp. 2807.
2. S. Skupsky, *et al.*, "Improved laser-beam uniformity using the angular dispersion of frequency-modulated light," J. Appl. Phys., vol. 66, 1989, pp. 3456-3462.
3. H. T. Powell, S. N. Dixit, M. A. Henesian, "Beam-smoothing capability on the Nova laser," ICF Quarterly Report, Lawrence Livermore National Laboratory, Livermore, CA, vol. 1, 1991, pp. 28-38.
4. M. A. Henesian, *et al.*, "Broadband laser amplification and beam smoothing by spectral dispersion in high power solid state lasers," *IQEC Technical Digest*, vol. 9, 1992, paper TuE3.
5. D. M. Pennington, *et al.*, "Effect of bandwidth on beam smoothing and frequency conversion at the third harmonic of the Nova laser," Proc. Soc. Photo-Instrum. Eng., vol. 1870, 1993, pp. 175-185.
6. W. L. Kruer, *The Physics of Laser Plasma Interactions*. New York: Addison-Wesley, 1988.
7. J. F. Drake, *et al.*, Phys. Fluids, vol. 17, 1974, pp. 1778.
8. R. L. Berger, "Supression of parametric instability by weakly incoherent laser beams," Phys. Rev. Lett., vol. 65, 1990, pp. 1207-1210.
9. P. J. Wegner, *et al.*, Applied Optics, vol. 31, 1992, pp. 6414-6426.
10. V. D. Volosov, *et al.*, "Method for compensating the phase-matching dispersion in nonlinear optics," Sov. J. Quantum Electron., vol. 4, 1975, pp.1090-1098.
11. V. D. Volosov and E. V. Goryachkina, "Compensation of phase-matching dispersion in generation of nonmonochromatic radiation harmonics.1. Doubling of neodymium-glass radiation frequency under free-oscillation condition," Sov. J. Quantum Electron., vol. 6, 1976,pp.854-857.
12. O. E. Martinez, "Achromatic phase matching for second harmonic generation of femtosecond pulses," IEEE J. Quantum Electron., vol. QE-25, 1989, pp. 2464-2468.
13. R. W. Short and S. Skupsky, "Frequency conversion of broad-bandwidth laser light," IEEE J. Quantum Electron., vol. QE-26, 1990, pp. 580-588.
14. M. D. Skeldon, *et al.*, "Efficient harmonic generation with a broad-band laser," IEEE J. Quantum Electron. , vol. QE-28, 1992, pp. 1389-1399.
15. R. S. Craxton, *et al.*, "Basic properties of KDP related to the frequency conversion of 1 mm laser radiation," IEEE J. Quantum Electron. , vol. QE-17, 1981, pp. 1782-1786.
16. M. S. Pronko, *et al.*, IEEE J. Quantum Electron. , vol. QE-26, 1990, pp. 337-347.
17. A. Peck and D. Milam, private communication, July, 1993.